Polym. Bull. (2012) 69:49–61
DOI 10.1007/s00289-011-0691-9

ORIGINAL PAPER

Solvent-driven reorganization of poly(diphenylacetylene) in film and nanofiber by means of swelling method: solvent annealing effects on fluorescence emission properties and microstructures

Dong-Hee Han · Wang-Eun Lee · Suk-Joon Kim · Su-Dong Park · Giseop Kwak

Received: 5 July 2011 / Revised: 16 November 2011 / Accepted: 12 December 2011 /
Published online: 21 December 2011

Abstract Freeze-dried nanofiber (Fr-nanofiber), spin-coated film (Sp-film), and solvent-cast film (So-film) of poly[1-phenyl-2-(*p*-trimethylsilyl)phenylacetylene] (PTMSDPA) were prepared to investigate solvent-annealing effects on their FL emission properties and microstructures by the swelling method. Their FL emission bands at maximum intensity ($\lambda_{max,FL}$) appeared at 525, 535, 540 nm, respectively. Their FL emission life times (τ_{avr}) were 0.489, 0.136, 0.130, respectively. In polarizing optical microscopy (POM) observation, the So-film showed a chevron texture on the surface, whereas Sp-film did not display any characteristic texture. The polarizing fluorescence microscopy images of the So-film converted in shadow when the polarizer angle changed from 0° to 90°. In XRD patterns, So-film showed a very sharp signal at a small angle of 6.9° with a corresponding lamellar layer distance of about 13 Å, whereas Sp-film did not show a sharp signal at the same angle. The FL intensity of PTMSDPA after annealing with ethanol under very slow evaporation more greatly decreased in turns of Fr-nanofiber (I/I_0 0.38), Sp-film (I/I_0 0.47), So-film (I/I_0 0.86). FL emission spectra of Sp-film annealed with ethanol, hexane, and methanol under very slow evaporation were measured. Ethanol (I/I_0 0.47) induced a greater decrease in FL emission intensity as compared to hexane (I/I_0 0.78) and methanol (I/I_0 0.65). POM, FL optical microscopy (FOM), and transmission electron microscopy (TEM) images as well as XRD patterns of

Electronic supplementary material The online version of this article (doi: 10.1007/s00289-011-0691-9) contains supplementary material, which is available to authorized users.

D.-H. Han · S.-J. Kim · S.-D. Park
Korea Electrotechnology Research Institute, 28-1 Seongju-dong, Changwon-si, Gyeongsangnam-do 641-120, Korea

W.-E. Lee · G. Kwak (✉)
Department of Polymer Science, Kyungpook National University, 1370 Sankyuk-dong, Buk-ku, Daegu 702-701, Korea
e-mail: gkwak@knu.ac.kr

Sp-film after ethanol annealing under slow evaporation were observed. The POM images and XRD patterns did not show any significant changes after solvent annealing while the FOM and TEM images certainly showed a little change. The FL emission of the film was weaker in the annealed part than in the non-annealed part. The annealed film exhibited several domains with certain lattice fringes of *d* space of $\sim$3.6 Å, while the as-prepared film showed exclusively amorphous regions.

Keywords Solvent annealing · Fluorescence · Poly(diphenylacetylene) · Swelling

Introduction

Intermolecular weak interactions, including hydrogen bonding, π–π interactions, Van der Waals forces, and London dispersion forces, intrinsically influence the microstructure and physical properties of a polymer in the solid state. Especially, for electron-rich, π-conjugated polymers with coplanar rigid backbone skeletons, the intermolecular stack structure formed by interchain π–π interactions is a very important factor in determining electrical and photophysical properties in the solid state [1, 2]. To date, conjugated polymers have been developed for various optoelectric applications as thin-film organic devices of light-emitting diode (LED) [3, 4], field effect transistor (FET) [5–7], and photovoltaic cell [8, 9], and so on. Their device performances, such as emission efficiency, charge mobility, and power conversion efficiency, respectively, have been remarkably enhanced by reorganization methods such as thermal annealing.

Thermal annealing is the most universal method to lower the entropy energy of polymer chains to achieve the most favorable chain-packing structure. This technique is easily applicable to crystalline and/or thermotropic liquid crystalline polymers with distinct phase transition temperatures. On the other hand, solvent-annealing method may be available in lyotropic liquid crystalline polymers with a high molecular weight (relatively low critical concentration) and a rigid backbone (high intrinsic viscosity). Especially, solvent annealing may be greatly effective for highly porous polymers as the solvent vapors and liquids can readily diffuse into the solids through the many microvoids. However, only a few examples of solvent annealing of π-conjugated polymers have been reported. The annealing effect and its mechanism have not been systematically studied to date [10, 11].

Disubstituted acetylene polymers are well known as amorphous, glassy polymers. Recently, we found that diphenylacetylene polymer derivatives show lyotropic liquid crystallinity in solution with a relatively low critical concentration, due to its ultra-high molecular weight (M_w) of $>1.0 \times 10^6$ and the main chain rigidity [12, 13]. Moreover, these polymers exhibit intense fluorescence (FL) in a wide visible range from sky blue to greenish yellow according to side alkyl chain length [13]. This unusual FL emission was assumed to be based on effective exciton confinement within the main chain due to the steric hindrance and/or intramolecular electron interactions of the bulky aromatic rings in the side chain groups [14, 15]. Tang and co-workers [16, 17] clarified the idea that the FL emission of dipenylacetylene polymers originates

Structure 1 Chemical structure of PTMSDPA

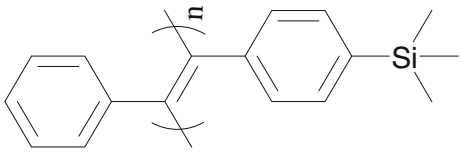

from the intramolecular excimer due to face-to-face stacking of the side phenyl rings. Further, we found that the stack degree of the side phenyl groups varies greatly according to the lamellar layer distance and the substitution position in the side phenyl ring [13, 18]. Among these polymer derivatives, poly[1-phenyl-2-(*p*-trimethylsilyl)phenylacetylene] (PTMSDPA in Structure 1) has the largest fractional free volume (FFV) of about 0.26 [19]. Notably, swelling out the polymer film with non-solvents leads to variation in the intramolecular phenyl–phenyl stack structure, which changes its FL emission properties [20]. Indeed, this polymer made for various kinds of liquid chemicals to rapidly diffuse into its film within subsecond, simultaneously, leading to a remarkable emission enhancement [21–23]. As mentioned above, in a respect of reorganization of the polymer chains in solid state, this swelling method may be used to achieve optimal chain-packing structure. However, the FL emission properties and microstructures after evaporation of the diffused solvents have been overlooked in our previous research. Detailed investigation of the annealing effect is very important for the use of PTMSDPA in various optical/electronic devices applications. In this study, spin-coated film (Sp-film), solvent-cast film (So-film), and freeze-dried nanofiber (Fr-nanofiber) were prepared using PTMSDPA. Their FL emission properties were investigated in comparison with each other. Further, solvent annealing effects on FL emission properties and microstructures were investigated by the swelling method. Especially, Sp-film was investigated in detail by FL emission and X-ray diffraction (XRD) spectroscopy as well as FL optical (FOM), polarizing optical (POM), polarizing fluorescence (PFM), and transmission electron microscopy (TEM).

Experimental section

Materials

PTMSDPA was donated from NOF Co. Ltd., Japan and was used as received. The synthetic method has been well described in previous articles [24, 25]. The solvents used in this study were purchased in spectrophotometric grade from Sigma-Aldrich Co. Ltd. or TCI Co. Ltd. with purity higher than 99%.

Sample preparation

Spin-coated film

PTMSDPA polymer was dissolved in toluene (concentration 0.5 wt%) to prepare a thin film on a glass slide (Matsunami) by spin-coating method (MDIAS Spin-1200D, 800–1,500 rpm).

Solvent-cast film

PTMSDPA polymer was dissolved in toluene (concentration 1.0 wt%) to prepare a thick film on a glass slide by solvent-casting method.

Freeze-dried nanofiber

PTMSDPA solution with a concentration of 0.003 wt% in benzene was prepared as previously described. Approximately 3 mL of solution was put into vials to be frozen in liquid nitrogen at −196 °C, after which the frozen samples were dried at −50 °C under 9 mm torr in a freeze dryer (Freeze dryer, Ilshin FD5505, Korea) for 24 h [26].

Measurements

The weight-average molecular weight (M_w) and number-average molecular weight (M_n) of PTMSDPA were evaluated by gel permeation chromatography [GPC, Shimadzu A10 instruments, Polymer Laboratories, PLgel Mixed-B (300 mm in length) as a column, and HPLC-grade tetrahydrofuran as an eluent at 40 °C], based on a calibration with polystyrene standards. FOM, POM, and PFM images were recorded on a Nikon Eclipse E600 fluorescence microscope equipped with a Nikon DS-Fi1 digital camera and a super-high-pressure 100-W Hg lamp (OSRAM, HBO103W/2). Irradiation power was controlled using several neutral density (ND) filters and was monitored by a UV-light meter (Lutron, YK-34UV). The FL images were taken with a Cannon PowerShot A2000IS. FL emission spectra were recorded on a JASCO ETC-273 spectrofluorometer at room temperature. To measure exciton lifetimes, time-correlated single photon counting (TCSPC) was performed. The second harmonic (SHG = 420 nm) of a tunable Ti:sapphire laser (Mira900, Coherent) with ~150 fs pulse width and 76 MHz repetition rate was used as an excitation source. The PL emission was spectrally resolved by using some collection optics and a monochromator (SP-2150i, Acton). The TCSPC module (PicoHarp, PicoQuant) with a MCP-PMT (R3809U, Hamamatsu) was used for ultrafast detection. The total instrument response function (IRF) for PL decay was <150 ps, which provided a temporal resolution of <10 ps. The deconvolution of actual FL decay and IRF was performed by using a fitting software (FlouFit, PicoQuant) to deduce the time constant associated with each exponential decay. XRD measurements were performed at room temperature using a X-ray diffracter (PANalytical X'Pert PRO-MPD) at the Korea Basic Science Institute (Daegu). The samples were mounted directly into the diffracter. The experiment was carried out by applying Cu Kα (1.54 Å) radiation at 40 kV and 25 mA. TEM imaging was performed on a Hitachi H-7600 instrument operated at 100 kV. All images were acquired using an AMT camera system.

Results and discussion

In general, polymer chains are completely isolated in ideal solution, whereas their mobility is highly restricted in the solid state. During film and fiber preparation, wet

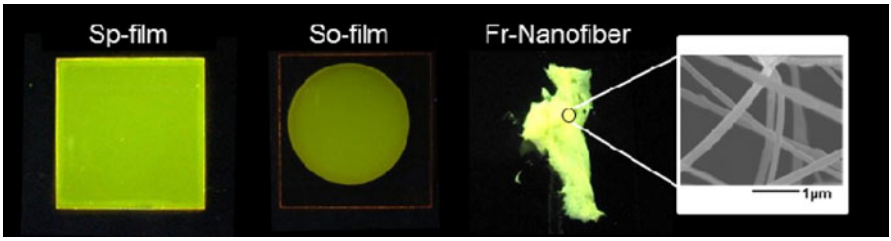

Fig. 1 Features of the Sp-film, So-film, and Fr-nanofiber (excited at >365 nm). *Inset* scanning electron microscope (SEM) image

processes necessarily cause a change in phases from solution to solid states. When this happens, the polymer chains may undergo different organization hysteresis according to the solidification method. There are two general methods to prepare polymer films. One is the solvent-casting method while the other is spin-coating technique. The latter is preferable to produce thin films with thicknesses of <1 μm. Nanofibers can be obtained by freeze-drying methods [26]. Moreover, if polymers do not need to be figurated after solidification, we can easily obtain bulk solids by quenching the polymer chains in non-solvents through precipitation. In this study, we prepared Sp-film (∼300 nm in thickness, toluene as a solvent), So-film (∼30 μm in thickness, toluene as a solvent), and Fr-nanofiber (∼50 nm in diameter, prepared as reported previously, cyclohexane as a solvent) using PTMSDPA with a high weight-average molecular weight of 5.23×10^6 g/mol and a polydispersity index of 3.2. Figure 1 shows the features of the as-prepared solid materials. As shown in the figure, their macroscopic appearances and FL emissions were different from each other. The polymer–solvent phase separation during fabrication of these featured materials was presumably influenced by the process conditions, including ambient temperature and solvent properties. Phase separation may also result in completely different chain-packing structures in the final products according to the type of solvent. The chemical affinity of a solvent to polymer should vary according to the type of solvent, i.e., whether the solvent is "aromatic or aliphatic" and/or "hydrophilic or hydrophobic" and/or "heavy or light", etc. Further, the solvent evaporation rate should vary according to the solidification method applied to the polymer solutions. Thus, the solidification method and conditions may determine the photophysical/electrical properties of the final products as well as the morphology and chain-packing structures. To confirm this, we conducted spectroscopic and microscopic analyses of all film and fiber samples. The details are described hereafter.

Figure 2 shows the normalized FL emission spectra of the as-prepared solid materials of Fr-nanofiber, Sp-film, and So-film. Their FL emission bands at maximum intensity ($\lambda_{max,FL}$) appear at 525, 535, 540 nm, respectively. Their FL emission life times (τ_{avr}) are 0.489, 0.136, 0.130, respectively. The "frozen-in" quenching of a polymer solution at an extremely low temperature of −196 °C essentially provides a highly coarsened structure in the nanofiber [26]. Accordingly, the polymer chains within the Fr-nanofiber may have contained incompletely stacked side phenyl rings in a disordered structure. On the other hand, the slower

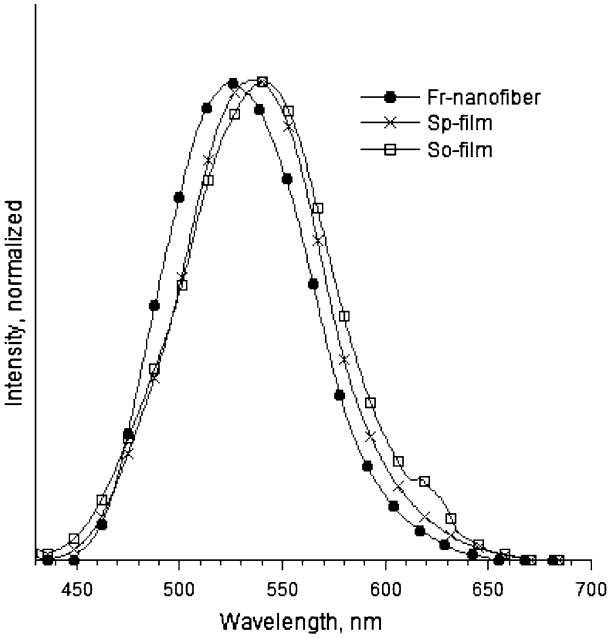

Fig. 2 Normalized FL emission spectra of Sp-film, So-film, and Fr-nanofiber (excited at 420 nm)

evaporation of toluene in the solvent-casting process may have more readily induced self-assembly of the polymer chains due to intrinsic liquid crystallinity, leading to relatively well-ordered chains with highly stacked side phenyl rings. Since solvent evaporation is much faster in the spin-coating process than casting process, the polymer chains within the Sp-film may be hardly ever organized. Accordingly, it is expected that the film- and fiber-preparation method significantly influences not only the photophysical properties but also the ordered structure of the polymer chains.

Actually, the differences in solvent evaporation time between the spin-coating and casting methods resulted in a significant difference in surface morphology

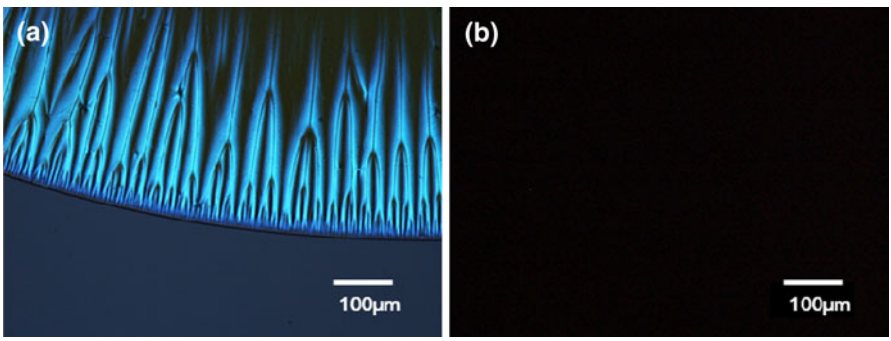

Fig. 3 POM images of **a** So-film and **b** Sp-film

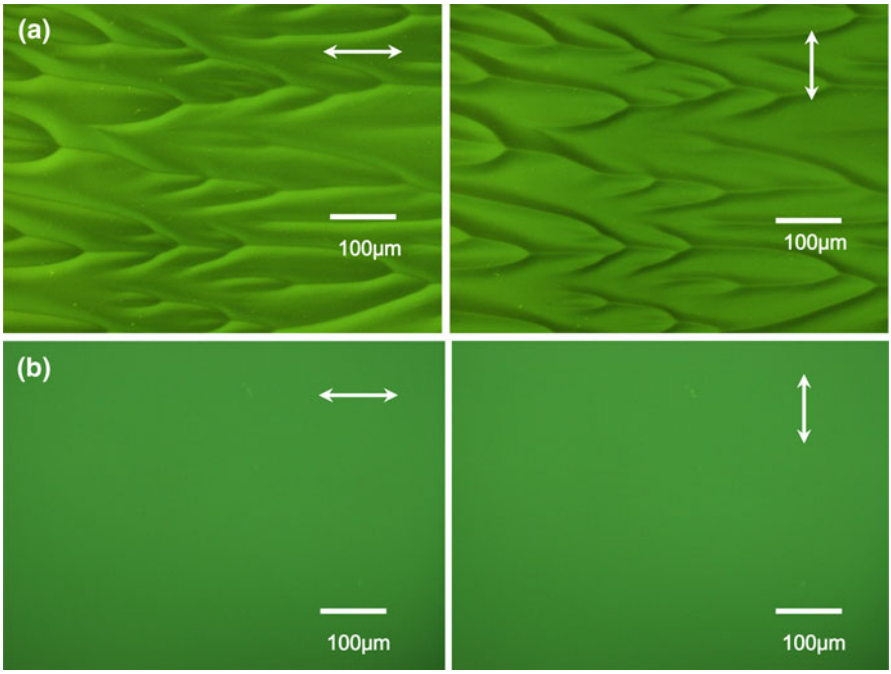

Fig. 4 PFM images of the **a** So-film and **b** Sp-film (excited at 365 nm)

between the Sp- and So-films. The Sp-film was completely isotropic while the So-film was anisotropic. Figure 3 shows the POM images of the Sp- and So-films. The So-film shows a texture with chevron morphology on the surface, whereas Sp-film does not display any characteristic texture. The solvent-casting experiment was conducted at a laboratory with not equipped with a constant temperature control system. When this experiment (solvent:toluene; concentration: 1 wt%) was conducted in a cold season of winter, the anisotropic texture well appeared. However, the characteristic texture hardly appeared with using a same solution in a warm season of summer. This indicates that the solvent evaporation rate significantly influences the surface morphology of the final film product in the casting process of PTMSDPA solution. A birefringent texture as chevron morphology is characteristic of a smectic phase due to a lamellar layer [23], indicating that a certain highly ordered structure was spontaneously formed via critical concentration point during slow solvent evaporation. The reason why Sp-film did not show a characteristic anisotropic texture is because the solvent evaporation was too fast for the polymer chains to self-organize during the extremely fast-spinning process. Moreover, as shown in Fig. 4, the PFM images of the So-film converted in shadow when the polarizer angle changed from 0° to 90° while the Sp-film did not. Figure 5 shows the XRD patterns of the Sp- and So-films. As already reported in a previous article, So-film shows a very sharp signal at a small angle of 6.9° with a corresponding lamellar layer distance of about 13 Å [13], whereas Sp-film does not show a sharp signal at the same angle. These POM, PFM,

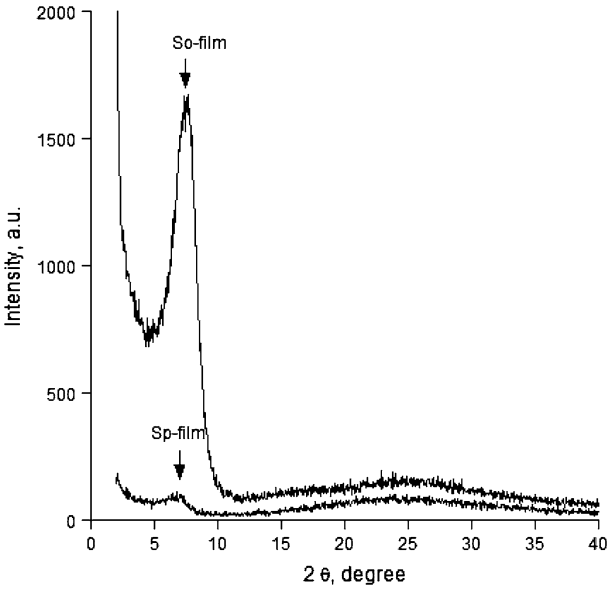

Fig. 5 XRD patterns of Sp- and So-films

and XRD results indicate the better-constructed structure of the polymer chains in So-film rather than Sp-film.

Figure 6 shows variations in the FL emission spectra of the Fr-nanofiber, Sp-film, and So-film upon solvent annealing with ethanol under very slow evaporation. The FL intensity of PTMSDPA after annealing more greatly decreased in turns of Fr-nanofiber (I/I_0 0.38) > Sp-film (I/I_0 0.47) > So-film (I/I_0 0.86), where I_0 and I are FL intensity before and after annealing, respectively. As mentioned previously, the side phenyl stack structure in the as-prepared Fr-nanofiber remains incomplete due to the quick "frozen-in" quenching of the polymer chains during spinodal decomposition at an extremely low temperature of −196 °C, whereas the as-prepared So-film provides well-ordered polymer chains with highly stacked side phenyl rings in response to self-assembly organization due to slow solvent evaporation and the intrinsic liquid crystallinity of the polymer. Further, the polymer chains are less densely packed in Sp-film than in So-film. In general, the higher the degree of aromatic stacking in a fluorophore molecule, the less intense the emission, due to an increase in excimer emission. Accordingly, the reorganization of the polymer chains in the solvent-driven disorder-to-order phase transition should be more apparent in turns of Fr-nanofiber > Sp-film > So-film. This should be responsible for the difference in I/I_0 values of the three different types of solid products.

We further investigated the effects of solvent annealing on the FL emission properties of Sp-film using various solvents. Figure 7 shows variations in the FL emission spectra of Sp-film upon annealing with ethanol, hexane, and methanol under very slow evaporation. A drop of ethanol was directly contacted to the surface

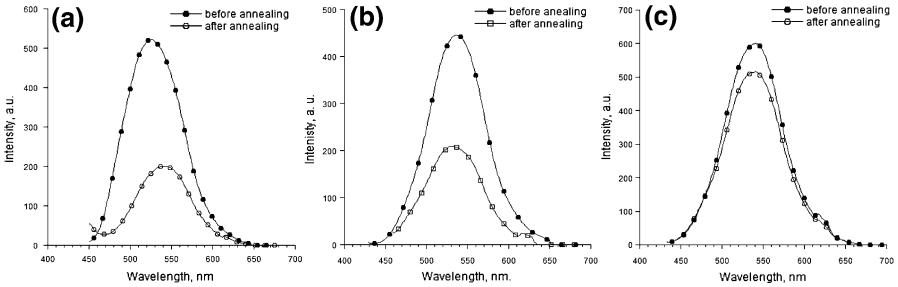

Fig. 6 Variations in FL emission spectra of **a** Fr-nanofiber, **b** Sp-film, and **c** So-film upon ethanol annealing under slow evaporation (excited at 420 nm)

of the solid material on glass slide and then chalet cap was covered on the glass slide at room temperature to slowly evaporate. Ethanol (I/I_0 0.47) induced a greater decrease in FL emission intensity as compared to hexane (I/I_0 0.78) and methanol (I/I_0 0.65). This was probably due to the fact that ethanol (saturated vapor pressure at 20 °C: 44.6 mmHg; boiling point: 78 °C) evaporates more slowly than hexane (120 mmHg; 69 °C) and methanol (96.2 mmHg; 64.6 °C). Namely, the polymer chains swollen in ethanol had enough time to reorganize themselves to achieve an optimal stack structure of the side phenyl rings, whereas hexane and methanol did not allow enough time for the polymer chains to be reorganized. Therefore, the greater decrease in FL emission corresponds to a greater increase in the degree of intramolecular phenyl–phenyl stacking. Further, it should be noted that, when the film was annealed at a faster evaporation rate, the FL intensity was not decreased as much relative to slow annealing. For example, the I/I_0 value of Sp-film was 0.67 during rapid annealing with ethanol (Fig. S1 in Supporting information). Moreover, the FL emission properties in rapid annealing were mainly dependent on the chemical affinity of the solvent to the polymer rather than the saturated vapor pressure and boiling point of the solvent. Hexane induced a much greater decrease in FL intensity relative to ethanol annealing (data was not shown). This was probably due to the fact that the chemical affinity to hydrophobic PTMSDPA is greater in hexane than in ethanol.

As previously shown in Fig. 3a, a semi-flexible polymer such as PTMSDPA tends to spontaneously lower its entropy energy by constructing a certain ordered structure via intermolecular weak interactions, resulting in liquid crystalline phases in So-film. We thus hypothesized that spontaneous reorganization could also be achieved even in isotropic Sp-film through disorder-to-order phase transition by the solvent-annealing method. To confirm this, we observed POM, FOM, and TEM images as well as XRD patterns of Sp-film after ethanol annealing under slow evaporation. However, the POM images and XRD patterns did not show any significant changes after solvent annealing. The POM image still displayed an isotropic texture, and birefringent texture was not observed after solvent annealing. Further, no sharp diffraction peak appeared in the XRD pattern after annealing (Fig. S2 in Supporting information). This may be attributed to the fact that the polymer chains could not be untangled or reorganized due to physical cross-linking

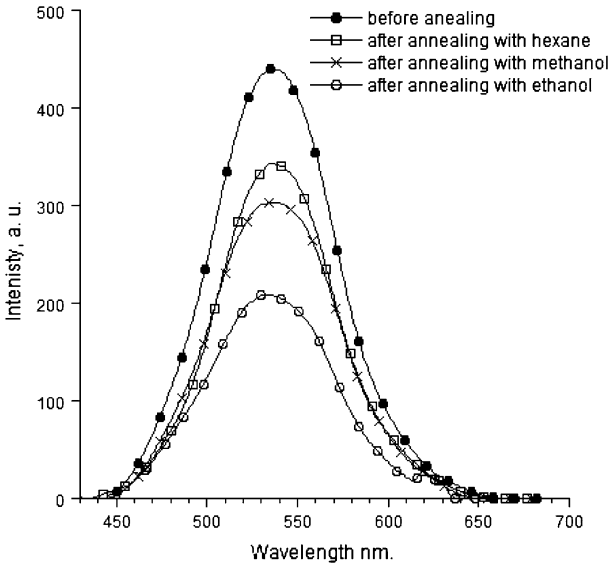

Fig. 7 Variations in FL emission spectra of Sp-film upon annealing with various solvents under slow evaporation (excited at 420 nm)

caused by the extremely high molecular weight of more than 1 million. Although no significant change was observed in the POM images and XRD pattern after solvent annealing, the FOM and TEM images certainly showed a little change. The details are described later.

Figure 8 shows FOM images and digital camera FL photographs of the Sp-film before and after ethanol annealing under slow evaporation. The FL emission of the film is weaker in the annealed part (right side) than in the non-annealed part (left side). This corresponds with the results from the FL emission spectroscopy, as

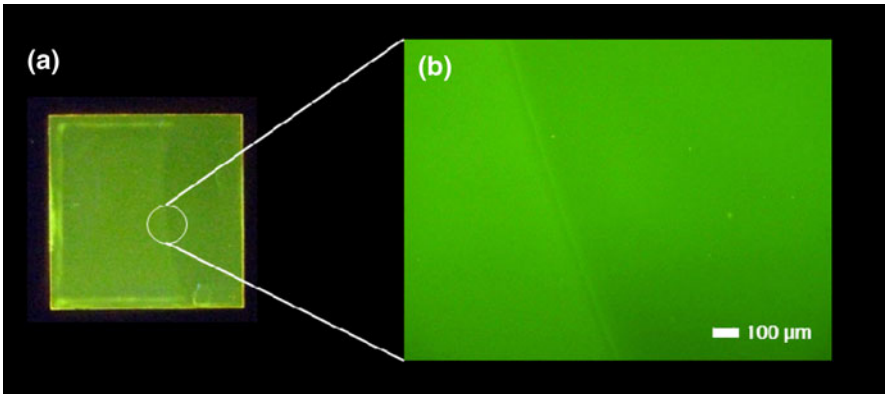

Fig. 8 **a** Digital camera FL photographs and **b** FOM images of Sp-film before and after ethanol annealing under slow evaporation (excited at 365 nm)

shown in Fig. 6b. The border between the annealed and non-annealed regions is clearly distinguishable. The reason why a change was observed in the FOM images but not in the POM and XRD analyses is because FL quenching could be amplified by a cooperative conjugation effect although the polymer chains underwent very minute conformational changes so as to be negligible.

The TEM study provided clear evidence about the partial changes in Sp-film. Figure 9 shows high-resolution TEM images of the Sp-film before (a, c) and after (b, d) ethanol annealing under slow evaporation. The annealed film exhibited several domains with certain lattice fringes of d space of $\sim$3.6 Å probably due to the incidentally aligned polymer chain domains (Fig. 9d). On the other hand, the as-prepared film showed exclusively amorphous regions (Fig. 9c). Although this disorder-to-order phase transition was not as remarkable as the thermally induced phase transition in the thermotropic liquid crystalline, rigid rod-like polymer

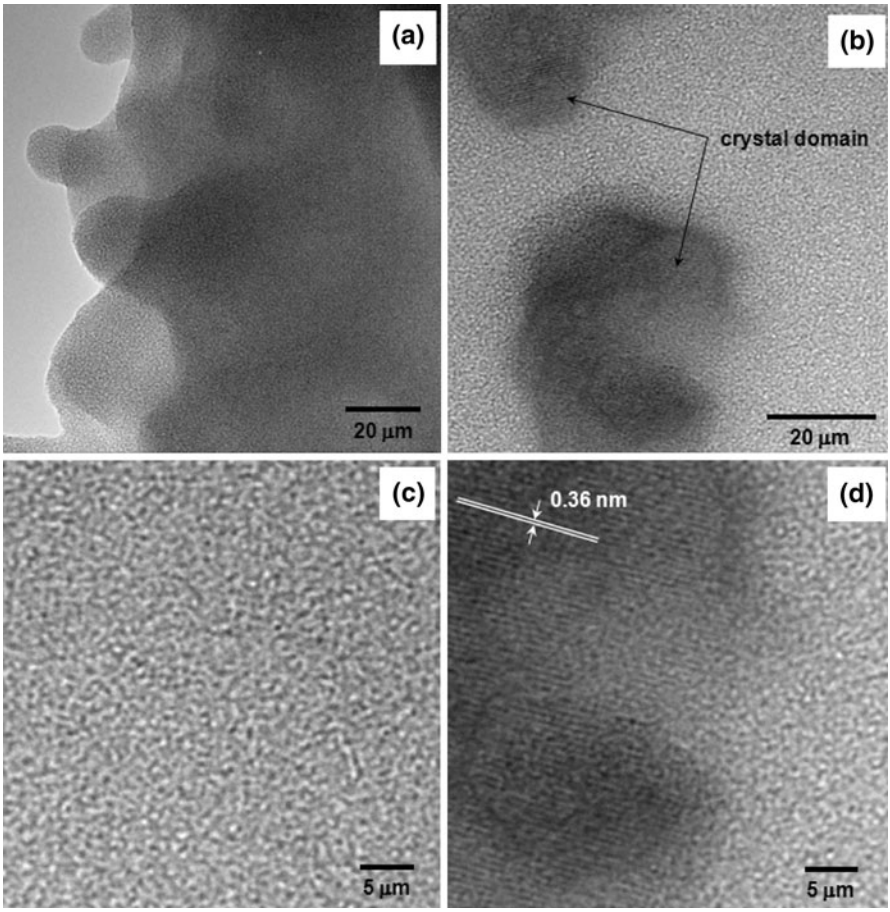

Fig. 9 High-resolution TEM images of Sp-film **a** before and **b** after solvent annealing with ethanol under slow evaporation. The film was obtained by spin coating the toluene solution of PTMSDPA on a copper grid. **c** and **d** are magnified images of **a** and **b** in part, respectively

derivatives [5–7], the crystalline domains gradually increased while the domain size grew bigger with an increase in the solvent contact time. This indicates that the polymer chains in the Sp-film partially form a certain ordered structure through solvent-driven reorganization.

Conclusions

We investigated solvent-annealing effects on FL emission properties and microstructures of PTMSDPA in Sp-film, So-film, and Fr-nanofiber in detail by the swelling method. The macroscopic appearances and FL emissions of as-prepared fiber and films were different from each other. The process conditions, including ambient temperature and the type of solvent, significantly influenced polymer–solvent phase separation, resulting in completely different chain-packing structures. FL emission, XRD, FOM, POM, PFM, and TEM studies revealed that solvent annealing of the fiber and films significantly influences their FL emission properties and microstructures as well as the morphology. Our result is expected to be helpful for understanding the solvent-driven reorganization mechanism of poly(diphenylacetylene) derivatives in fiber and film.

Acknowledgments The authors sincerely thank NOF Co., Ltd., Japan, for the donation of PTMSDPA. This study was supported by the Basic Science Research Program through National Research Foundation of Korea (NRF) grants funded by the Korea government (MEST) (2011-0001082, 2011-0004045, 2011-0016681). The authors acknowledge financial support in the form of a grant from the Korea Electrotechnology Research Institute. This study was supported by the R&D program for Energy & Resource Technology funded by the Ministry of Knowledge Economy.

References

1. Bunz UHF (2000) Poly(aryleneethynylene)s: syntheses, properties, structures, and applications. Chem Rev 100(4):1605
2. Grenier CR, Pisula W, Joncheray TJ, Muller K, Reynolds JR (2007) Regiosymmetric poly(dialkylphenylenedioxythiophene)s: electron-rich, stackable-conjugated nanoribbons. Angew Chem Int Ed 46(5):714
3. Nguyen TQ, Kwong RC, Thompson ME, Schwartz BJ (2000) Improving the performance of conjugated polymer-based devices by control of interchain interactions and polymer film morphology. Appl Phys Lett 76(17):2454
4. Ahn JH, Wang C, Widdowson NE, Pearson C, Bryce MR, Petty MC (2005) Thermal annealing of blended-layer organic light-emitting diodes. J Appl Phys 98(5):054508
5. Bao Q, Li J, Li CM, Dong ZL, Lu Z, Qin F, Gong C, Guo J (2008) Direct observation and analysis of annealing-induced microstructure at interface and its effect on performance improvement of organic thin film transistors. J Phys Chem B 112(39):12270
6. Kim DH, Lee BL, Moon H, Kang HM, Jeong EJ, Park JI, Han KM, Lee S, Yoo BW, Koo BW, Kim JY, Lee WH, Cho K, Becerril HA, Bao Z (2009) Liquid-crystalline semiconducting copolymers with intramolecular donor-acceptor building blocks for high-stability polymer transistors. J Am Chem Soc 131(17):6124
7. Bao Z, Dodabalapur A, Lovinger AJ (1996) Soluble and processable regioregular poly(3-hexylthiophene) for thin film field-effect transistor applications with high mobility. Appl Phys Lett 69(26):4108

8. Kim Y, Choulis SA, Nelson J, Bradley DDC (2005) Device annealing effect in organic solar cells with blends of regioregular poly(3-hexylthiophene) and soluble fullerene. Appl Phys Lett 86(6):063502
9. Li G, Shrotriya V, Huang J, Yao Y, Moriarty T, Emery K, Yang Y (2005) High-efficiency solution processable polymer photovoltaic cells by self-organization of polymer blends. Nat Mater 4(11):864
10. Lee WH, Kim DH, Choo JH, Jang Y, Lim JA, Kwak D, Cho K (2007) Change of molecular ordering in soluble acenes via solvent annealing and its effect on field-effect mobility. Appl Phys Lett 91(9):092105
11. Li G, Yao Y, Yang H, Shrotriya V, Yang G, Yang Y (2007) "Solvent annealing" effect in polymer solar cells based on poly(3-hexylthiophene) and methanofullerenes. Adv Funct Mater 17(10):1636
12. Kwak G, Minaguchi M, Sakaguchi T, Masuda T, Fujiki M (2007) Poly(diphenylacetylene) bearing long alkyl side chain via silylene linkage: its lyotropic liquid crystallinity and optical anisotropy. Chem Mater 19(15):3654
13. Kwak G, Minaguchi M, Sakaguchi T, Masuda T, Fujiki M (2008) Alkyl side-chain length effects on fluorescence dynamics, lamellar layer structures, and optical anisotropy of poly(diphenylacetylene) derivatives. Macromolecules 41(7):2743
14. Hidayat R, Tatsuhara S, Kim DW, Ozaki M, Yoshino K, Teraguchi M, Masuda T (2000) Time-resolved study of luminescence in highly luminescent disubstituted polyacetylene and its blend with poorly luminescent monosubstituted polyacetylene. Phys Rev B 61(15):10167
15. Shukla A (2004) Theory of two-photon absorption in poly(diphenyl) polyacetylenes. Chem Phys 300(1–3):177
16. Yuan WZ, Qin A, Lam JWY, Sun JZ, Dong Y, Haussler M, Liu J, Xu HP, Zhen Q, Tang BZ (2007) Disubstituted polyacetylenes containing photopolymerizable vinyl groups and polar ester functionality: polymer synthesis, aggregation-enhanced emission, and fluorescent pattern formation. Macromolecules 40(9):3159
17. Qin A, Jim CKW, Tang Y, Lam JWY, Liu J, Mahtab F, Gao P, Tang BZ (2008) Aggregation-enhanced emissions of intramolecular excimers in disubstituted polyacetylenes. J Phys Chem B 112(31):9281
18. Lee WE, Oh CJ, Park GT, Kim JW, Choi HJ, Sakaguchi T, Fujiki M, Nakao A, Shinohara KI, Kwak G (2010) Substitution position effect on photoluminescence emission and chain conformation of poly(diphenylacetylene) derivatives. Chem Commun 46(35):6491
19. Toy LG, Nagai K, Freeman BD, Pinnau I, He Z, Masuda T, Teraguchi M, Yampolskii YP (2000) Pure-gas and vapor permeation and sorption properties of poly[1-phenyl-2-[*p*-(trimethylsilyl)phenyl]acetylene] (PTMSDPA). Macromolecules 33(7):2516
20. Lee WE, Kim JW, Oh CJ, Sakaguchi T, Fujiki M, Kwak G (2010) Correlation of intramolecular excimer emission with lamellar layer distance in liquid-crystalline polymers: verification by the film-swelling method. Angew Chem Int Ed 49(8):1406
21. Kwak G, Lee WE, Jeong H, Sakaguchi T, Fujiki M (2009) Swelling-induced emission enhancement in substituted acetylene polymer film with large fractional free volume: fluorescence response to organic solvent stimuli. Macromolecules 42(1):20
22. Kwak G, Lee WE, Kim WH, Lee H (2009) Fluorescence imaging of latent fingerprints on conjugated polymer films with large fractional free volume. Chem Commun 16:2112
23. Jeong H, Lee WE, Kwak G (2010) Enhancements in emission and chemical resistance of substituted acetylene polymer via in situ sol–gel reaction in film. Macromolecules 43(2):1152
24. Tsuchihara K, Masuda T, Higashimura T (1991) Tractable silicon-containing poly(diphenylacetylenes): their synthesis and high gas permeability. J Am Chem Soc 113(22):8548
25. Tsuchihara K, Masuda T, Higashimura T (1992) Polymerization of silicon-containing diphenylacetylenes and high gas permeability of the product polymers. Macromolecules 25(21):5816
26. Lee WE, Oh CJ, Kang IK, Kwak G (2010) Diphenylacetylene polymer nanofiber mats fabricated by freeze drying: preparation and application for explosive sensors. Macromol Chem Phys 211(17):1900